Applied Catalysis A: General 517 (2016) 30–38

Contents lists available at ScienceDirect

Applied Catalysis A: General

journal homepage: www.elsevier.com/locate/apcata

Pt supported nitrogen doped hollow carbon spheres for the catalysed reduction of cinnamaldehyde

Isaac Nongwe[a,c], Vilas Ravat[a], Reinout Meijboom[b], Neil J. Coville[a,*]

[a] DST-NRF Centre of Excellence in Strong Materials and Molecular Sciences Institute, School of Chemistry, University of the Witwatersrand, Johannesburg, WITS 2050, South Africa
[b] Department of Chemistry, University of Johannesburg, Johannesburg, Auckland Park 2006, South Africa
[c] Department of Civil and Chemical Engineering, University of South Africa, P/Bag X6, FL, Johannesburg 1710, South Africa

ARTICLE INFO

Article history:
Received 23 October 2015
Received in revised form 23 February 2016
Accepted 25 February 2016
Available online 2 March 2016

Keywords:
Nitrogen doped hollow carbon spheres
Silica template
Pt catalyst
Cinnamaldehyde reduction

ABSTRACT

Carbon and nitrogen coated Stöber silica spheres were prepared by a standard procedure using acetonitrile at different CVD temperatures (800–1000 °C) and as a function of time (1–4 h). HF treatment was used to remove the silica from the carbon coated silica to give monodispersed nitrogen doped hollow carbon spheres (N-HCSs; shell thickness = 50 nm). The surface areas of the N-CSs increased significantly after removal of the SiO_2 core (N-HCS = 47 m^2/g). Platinum nanoparticles, prepared by a [$Pt(COD)Cl_2$] deposition method were dispersed (d = 2.8 ± 0.4 nm) on the N-HCS supports. Thermal treatment of the Pt/N-HCS900-4 (prepared at 900 °C for 4 h) in a 5% H_2/Ar atmosphere at 120 °C (Pt/N-HCS900-4-120) and 300 °C (Pt/N-HCS900-4-300) gave metallic Pt (2.48%) which was confirmed by XRD and XPS studies. The XPS N1s spectra of Pt/N-HCS900-4-120 showed the presence of quaternary, pyridinic and pyrollic nitrogen atoms. These nitrogen doped carbon supported Pt nanoparticle catalysts were observed to reduce cinnamaldehyde to the unsaturated alcohol, cinnamyl alcohol (isopropanol/30 bar H_2/80 °C) with >99% conversion and selectivity. The catalyst used in the reduction of cinnamaldehyde to cinnamyl alcohol could be recycled 12 times with minimal loss in conversion and this correlated with the small amount of Pt leaching or physical loss of catalyst (<2%). The corresponding Pt/catalyst made on undoped HCSs showed a much greater loss of activity with recycling. It is seen that N doping of carbon is an effective method to bind Pt to carbon.

1. Introduction

Spherically shaped solid carbon materials have been known for decades. They have been well studied and characterised and their properties have been exploited for use in many areas (tyres, batteries, printer inks, supports for catalysis, medical probes etc) [1–7]. More recently a new class of spheres called hollow carbon spheres (HCSs) have been developed [8–11].

In most procedures the HCSs are made from a core shell structure in which the core comprised of a removable template material and the shell is made of carbon. Silica spheres are often used as the template, and the deposition of a carbon reactant on the template followed by subsequent removal of the template (HF [12], NaOH [13] etc.) produces the HCSs. Partial removal of the interior has led to egg/yolk or rattle materials [14]. In general, the structure of the resulting carbon material is an inverse replica of the silica template and the morphology of the silica template is retained in the carbon material [15]. Thus, by varying the size of the template, the size of the HCS can be varied. The carbon layer deposited on the template will be affected by the carbon containing reagent used to prepare the layer. By choice of the reaction conditions and the type of the carbon used the thickness of the layer can be controlled.

The surface of a carbon can be modified by functionalization or by doping. Dopants such as N, B, P and O when incorporated into a carbon structure will also tune the physicochemical properties of the carbon material i.e. doping on any shaped carbon material should give materials with properties different from their undoped analogues. Doping of HCSs can be expected to show similar behaviour [15].

Doping of HCSs can in principle be achieved by two major routes—*in situ* doping or post addition of an element to a HCS; typically with N as the dopant. Studies have been reported in which *in situ* N doping has been achieved from a variety of N sources. For example, NHCSs have been synthesized by hydrother-

* Corresponding author.
E-mail address: neil.coville@wits.ac.za (N.J. Coville).

http://dx.doi.org/10.1016/j.apcata.2016.02.025
0926-860X/

mal carbonization of poly(o-phenylenediamine), [16] pyrolysis of poly(o-phenylenediamine) [17], aminated tannins [18], ionic liquids [19] and pyrroles [20] as the precursors. The N-HCSs produced by hydrothermal methods result in amorphous carbon walls with low thermal stability and a low level of graphitization. Alternatively N-HCSs made by a high temperature CVD process e.g. using CH_3CN as N (and C) source gives HCSs with a more graphitic structure [13,21].

HCSs with a controlled size, shape, morphology and chemical composition, have received growing interest because of their potential applications in catalysis [3,16,22], gas storage [23], adsorption [24], drug delivery [25], and energy conversion [26–28]. As expected, N-HCSs can also be exploited in similar areas to those of HCSs [29]. Our own studies in this area relate to the use of doped HCSs as catalyst supports [30,31].

In a further exploration of these materials we wish to report on our studies using Pt/NHCS as a catalyst for the reduction of cinnamaldehyde. We have chosen to prepare our NHCSs using a CVD method as this method yields a more graphitic carbon with less oxygenated surface groups. The binding interaction between the carbon and the Pt should thus be predominantly influenced by the effect of the N dopant atoms.

Selective catalytic hydrogenation of α,β-unsaturated aldehydes is an important step in the industrial preparation of many fine chemicals and attracts much interest [32]. Reduction of cinnamaldehyde can lead to three different products: a saturated aldehyde, a saturated alcohol and the desired unsaturated alcohol (see reaction Scheme 1). When the reaction is performed in isopropanol as solvent other side products involving interaction with the solvent can form [33]. Cinnamyl alcohol plays an important role in the perfume and flavouring industries [34]. The hydrogenation of the C=C bond in α,β-unsaturated aldehydes is both kinetically and thermodynamically more favourable than the hydrogenation of the C=O group [35]. The most significant factors determining the selectivity are the presence of a catalyst, the type and the structure of the active metal, the characteristics of the catalyst particle (size/shape), the type of the support and the conditions of the reaction, e.g. the hydrogen pressure and the reaction temperature. The cinnamaldehyde reduction reaction thus provides an excellent model reaction to study new catalyst formulations.

Many studies have been reported on the use of catalysts for cinnamaldehyde reduction. Of the metals investigated Pt has proven to give excellent results and reported studies using Pt, especially on other carbon supports, provide good reference studies to evaluate the use of N-HCSs [36–49].

Here we use the CVD synthesis route to make N-HCSs. The ability of the N-HCS to act as a catalyst support was studied and the performance of a supported Pt catalyst was evaluated for the selective reduction of cinnamaldehyde to cinnamyl alcohol in isopropanol at different temperatures and hydrogen pressures. No promoter was used in the study.

2. Experimental

2.1. Synthesis of silica spheres

Monodisperse silica spheres with a diameter d = 1100 ± 100 nm were synthesized following a two-step modified Stöber procedure described elsewhere [50]. In this reaction, 22.4 mL of TEOS, 15.4 mL of 25% NH_3 solution, and 18 mL of deionised water were added into 130 mL of isopropanol and the mixture was aged for 1 h under mild stirring at 40 °C. A further 22.4 mL of TEOS was then added to the above reaction mixture which was stirred at room temperature overnight, resulting in the formation of a white silica colloidal suspension. The silica particles were centrifuged, separated and washed with ethanol and distilled water 4 times and dried at 80 °C for 12 h. Finally, they were sonicated for 15 min in a water and ethanol mixture to give well separated monodisperse silica spheres.

2.2. Preparation of hollow carbon spheres and preparation of catalysts

Deposition of carbon onto the large SiO_2 spheres (1100 nm) was carried out using a CVD bubbling method. A range of N containing reagents (acetonitrile, aniline, triethylamine and trimethylamine) were initially used as a carbon and nitrogen source to make the N-HCSs respectively but the acetonitrile gave the best results (see Supplementary material) [13]. Briefly, the silica spheres were placed in a quartz tube and were heated to 800, 850 or 900 °C for 4 h or 900 °C for 1–3 h at a heating rate of 10 °C/min under a N_2 flow (90 mL min^{-1}) at atmospheric pressure. During this time the silica spheres shrank and had diameters of 800 nm (800 °C), 750 nm (850 °C) and 705 nm (900 °C) respectively. Then, N_2, was bubbled through the acetonitrile and the vapours passed through a quartz tube reactor (20 cm × 2 cm) containing the silica spheres in order to allow carbon deposition to occur on the surface of the silica spheres. After a given period of time, a black composite consisting of carbon/silica spheres was obtained. Removal of the silica using 20 wt% HF solution (15 mL HF was added to 1.5 g carbon/silica composite and the mixture aged for 48 h) yielded a range of hollow carbon spheres: N-HCS800-4, N-HCS850-4 and N-HCS900-4 for samples made at 800, 850 and 900 °C for 4 h respectively, and N-HCS900-1, N-HCS900-2 and N-HCS900-3, for the samples made when carbon was deposited after 1–3 h at 900 °C.

A HCS sample without N was also prepared by depositing carbon from toluene onto silica spheres (HCS900-4).

2.3. Synthesis of [Pt(COD)Cl_2] and Pt/N-HCS catalyst

The complex [Pt(COD)Cl_2] was prepared by a method reported in the literature [51,52]. A solution of K_2PtCl_4 (2.5 g, 6.0 mmol) was prepared in H_2O (40 mL). Glacial acetic acid (60 mL) and 1,3-cyclo-octadiene (COD; 2.5 mL, 20 mmol) were added to the above solution. The reaction mixture was stirred in air and heated at 90 °C on a steam bath. After 30 min, the red solution turned pale yellow. The solution was allowed to cool and pale yellow crystals were isolated. The crystals were washed with H_2O, ethanol and diethyl ether. All spectroscopic data were in agreement with the literature values [51,52].

The [Pt(COD)Cl_2] (0.037 g) was dispersed in a solution of sodium citrate (4 mL) in deionized water (50 mL) containing hollow carbon spheres (1 g) and sonicated for 1 h. Then, 2 mL of 0.5 M $NaBH_4$ was introduced dropwise to the above suspension with vigorous stirring at room temperature. The mixture was left stirring overnight and the solid phase was recovered by filtration. It was washed with water and then thermally treated in an Ar/H_2 (5%) atmosphere at 120 and 300 °C (these samples were called Pt/N-HCS900-4-120 and Pt/N-HCS900-4-300). A Pt/HCS900-4-120 catalyst was also prepared to allow for comparison with the Pt/N-HCS900-4-120 catalyst. Four other catalysts were prepared by the same procedure as described above but using N-HCS800-4, N-HCS850-4, N-HCS900-1 and N-HCS900-2 as supports. The materials generated from the different N-HCSs heated at 120 °C in an Ar/H_2 (5%) atmosphere were called Pt/N-HCS800-4-120, Pt/N-HCS850-4-120, Pt/N-HCS900-1-120 and Pt/N-HCS900-2-120.

2.4. Catalytic reduction reaction

Liquid phase hydrogenation of cinnamaldehyde (98%, Aldrich) was carried out in a 100 mL stirred batch reactor (autoclave) under temperature control. The total volume in the teflon container

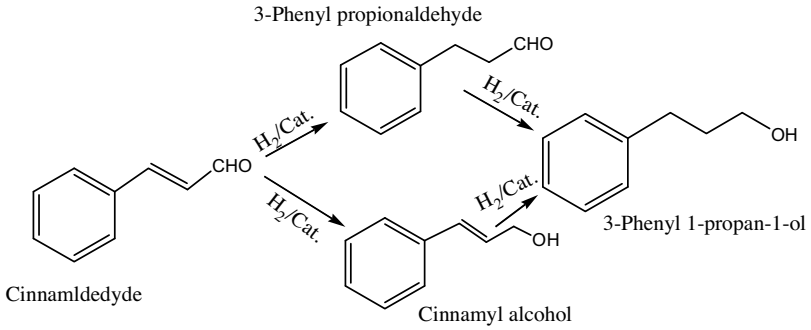

Scheme 1. Reaction network for the cinnamaldehyde hydrogenation reaction.

placed inside the autoclave was 35 mL. Reactions were performed under different pressures (10, 20 and 30 bar) and at different temperatures (20, 40, 60 and 80 °C). Prior to hydrogenation, the catalysts were activated under a hydrogen atmosphere at 120 °C (heating rate: 5 °C/min) for a period of 2 h. The reaction mixture containing cinnamaldehyde (5 mL), catalyst (0.2 g) and solvent (isopropanol, 30 mL) was placed in the teflon lined autoclave. To determine if any Pt leaching had occurred, a hot filtration test was used i.e. at the end of a catalytic reaction, the product mixture was filtered off and the solid catalyst remaining was washed with acetone and reused (or analyzed). The reaction products and unconverted reactants from the filtrate were analyzed by gas chromatography with an FID, using a capillary column (Phenomenex Zebron, 30 m × 0.53 mm I.D) and N_2 as the carrier gas. Appropriate standards were used to establish the identity of the GC peaks.

2.5. Catalyst characterization

Chemical analysis of the catalysts was performed using ICP-OES to measure the Pt concentration (Spectro Genesis instrument). Approximately 50 mg of catalyst was weighed and the carbon oxidised at 700 °C. Then the samples were dissolved in 5 mL HF, 4 mL HNO_3 and few drop of $HClO_4$. This procedure was repeated twice after the acid evaporation step. Finally, the residue was dissolved in *aqua regia* and heated until dryness and then an aqueous solution of HNO_3 (1% v/v) was added. The solution was transferred to a 50 mL volumetric flask for analysis. CN elemental analyses were performed with an Elementar Vario Micro cube analyser (Rhodes University, SA). A JEM 100s, an FEI Tecnai G^2 Spirit and an FEI Tecnai F20 X-Twin at 200 kV FEG with an Oxford EDS system were used for transmission electron microscopy (TEM) studies. All samples were ultrasonically suspended in methanol and a drop of the suspension was transferred to a copper grid and allowed to dry before TEM analysis. The number and diameters of the Pt particles and the NHCSs were determined by standard counting procedures from TEM images. The phase composition of the support and catalysts were determined by means of XRD analysis on a Bruker D2 phaser in Bragg Brentano geometry with a Lynxeye detector using Cu-Kα radiation at 30 kV and 10 mA. The scan range was $10° < 2\theta < 90°$ in 0.040 steps, using a standard speed with an equivalent counting time of 1 s per step. The diffraction peaks were then compared with those of standard compounds reported in the Diffracplus evaluation package using the EVA (V11.0, rev.0, 2005) software package. A PerkinElmer TG/DTA Thermogravimetric analyzer was used to measure weight changes of samples heated in air or nitrogen at a constant heating rate of 10 °C/min. The sample mass used was varied between 0.005 and 0.01 g. Scanning electron microscopy (SEM) images were recorded using a Philips XL-30 instrument coupled to an energy dispersion unit using an EDX Link Analytical QX-20000 system at an accelerator voltage of 5 kV. The samples were mounted on a copper stub with conductive carbon sticky tape. A thin (ca. 5 nm) coating of gold was deposited onto the samples to reduce the effects of charging. Raman spectra of the spent catalysts were obtained on a T64000 Raman spectrometer (Jobin Yvon triple spectrometer) under ambient conditions. A 514.5 nm Ar laser was used as the exciting source with a power density of 1 mW cm^{-2} on the sample surface and a power of 2 mW. The measurements were referenced to Si at 521 cm^{-1} with 16 data acquisitions in 180 s. A low laser power was used to prevent burning of the samples.

3. Results and discussions

3.1. Structure and morphology of the nitrogen doped N-HCS samples

3.1.1. Effect of CVD temperature

The silica spheres were prepared using a modified Stöber synthesis and after deposition of carbon and nitrogen, the silica was removed using HF. The SEM images (Fig. S1a) show monodisperse silica spheres with a narrow size distribution (d = 1100 ± 100 nm) and homogeneous shape. The silica spheres were placed in a CVD oven that was heated from room temperature to 800, 850 and 900 °C at 10 °C min^{-1} during which time the spheres shrank. N_2 (100 mL min^{-1}) was then bubbled through acetonitrile and this mixture was passed over the spheres at 800, 850 and 900 °C for 4 h. The material was shown by SEM and TEM analysis (Fig. S1a) to consist of accreted spheres with diameters of 825, 800 and 750 ± 50 nm respectively with a single shell and thickness between 25 and 50 ± 5 nm (see Table 1). The results indicate that a higher CVD temperature enhanced the carbon deposition rate, increased the shell thickness and the extent of silica shrinkage and promoted the formation of a smooth carbon surface. The N content was found to be 6.7, 7.2 and 8.6 wt% N for the N-HCS800-4, N-HCS850-4 and N-HCS900-4 spheres. The data shows that the nitrogen content increases with reaction temperature.

The N-HCS samples obtained at 800, 850 and 900 °C were studied by thermogravimetric analysis under air. Fig. S1b displays the TGA curves of these N-HCS samples. The sample prepared at the higher temperature showed the highest stability (Fig. S1). This data also correlates with the graphitic nature of the carbon as determined by Raman spectroscopy (Fig. S2).

3.1.2. Effect of CVD reaction time on the shell thickness of N-HCSs

The silica spheres (d = 1100 nm ± 100) were placed in a CVD oven heated at 900 °C (under N_2) while acetonitrile was passed over the spheres for different time periods to study the effect of time on the sphere size. The shell thickness and size as determined from SEM and TEM images increased continuously and the resultant carbon/silica composites after 1–4 h CVD time gave N-HCSs with shell thicknesses of 14, 20, 35 and 45 ± 5 nm respectively (Fig. 1). The samples studied at the different times had a N content of 8.4 (1 h), 8.5 (2 h), 8.6 (3 h) and 8.6 (4 h) wt% N respectively. Thus, the N con-

Table 1
BET surface areas and pore parameters of the N-HCS materials produced at different temperatures.

Sample	Temperature °C	Spheres size nm[b]	$S_{BETm}{}^2$/g	Pore volume cm^3g^{-1}
SiO_2	800	800	2.0	0.03
SiO_2	850	755	1.4	0.01
SiO_2	900	700	1.6	0.02
SiO_2@C	800	825	1.4	0.01
SiO_2@C	850	800	1.7	0.02
SiO_2@C	900	750	0.7	0.01
N-HCS800-4	800	–	59	0.30
N-HCS850-4	850	800	55	0.28
N-HCS900-4	900	750	47	0.22
Pt/N-HCS900−4-120[a]	–	750	35	0.18

[a] Pt/N-HCS900-4-120: pre-treated in H_2 (5%)/Ar (100 mL) at 120 °C for 2 h.
[b] ±50 nm.

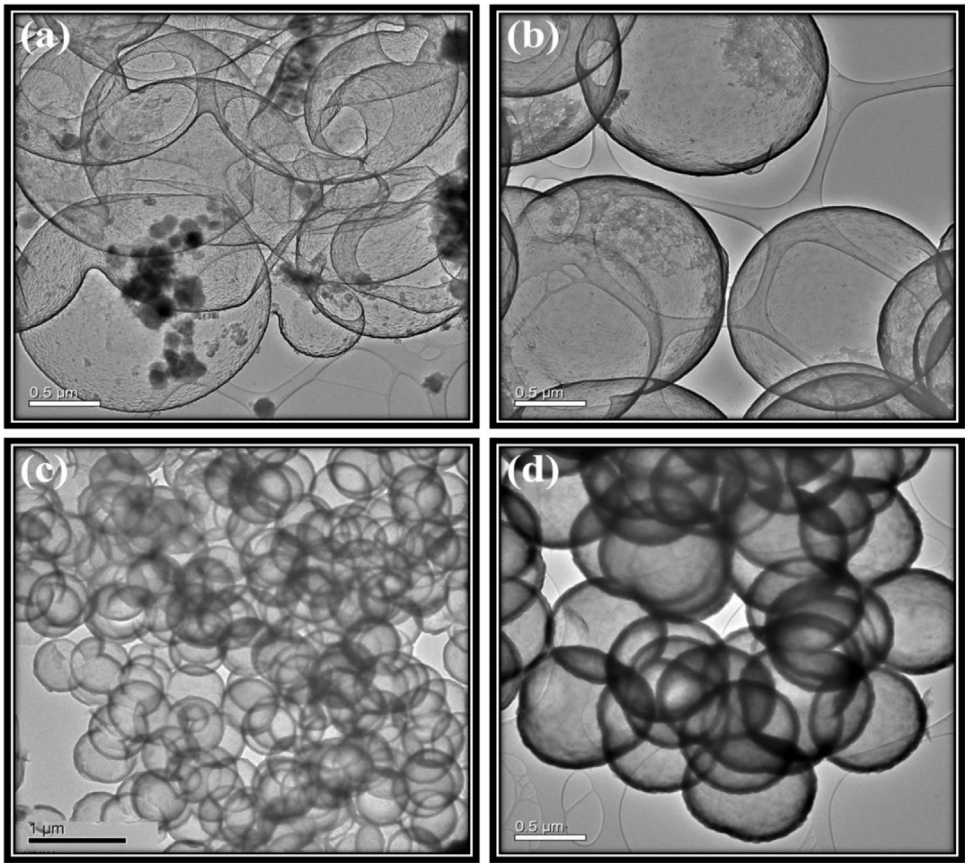

Fig. 1. TEM images of N-HCSs obtained from 1100 nm silica spheres after different CVD times for (a) N-HCS900-1, (b) N-HCS900-2, (c) N-HCS900-3 and (d) N-HCS900-4.

centration did not vary significantly with reaction time suggesting that the N was deposited in a homogeneous process into the carbon sphere.

3.1.3. *Structural parameters for the N-HCS material*

The nitrogen sorption data for silica spheres and silica/carbon composites after 4 h CVD at 800–900 °C gave low BET surface area values between 1 and 2 m^2/g. After silica etching from the silica/carbon composite, an increase in surface area was noted. The Brunauer-Emmett-Teller (BET) surface areas of N-HCS800-4, N-HCS850-4 and N-HCS900-4 materials were 59, 55 and 47 m^2/g respectively (Table 1). The decrease in BET value with increasing CVD temperature was due to the formation of a more porous carbon (N-doped) shell. Further, the carbon pieces and broken spheres formed at the lower synthesis reaction temperatures would also give a higher surface area material. Thus the conversion of the core-shell structures to the hollow structures leads to a successful enhancement in the carbon surface area. Thus the N-HCSs should provide a better catalyst support material (allowing for enhanced metal particle dispersion) relative to the SiO_2@C material.

Fig. 2 depicts the wide-angle diffraction pattern of samples that were carbonized at different temperatures. The diffraction peaks at $2\theta = 26$ and 43° (JCPDS Card File, No. 41–1487) corresponded to (0 0 2) and (1 0 0) reflections from the graphite phase. For the N-HCS800 sample, the (0 0 2) diffraction peak is relatively low in intensity and broad in shape. This suggests that the sample possesses a low degree of graphitization. This result is consistent with the TEM images (Fig. 1a) where broken N-HCSs were observed. As the temperature of carbonization increased from 800 to 900 °C, the sharpness of the carbon 002 diffraction peak was enhanced, indicating the positive effect of increasing carbonization temperature

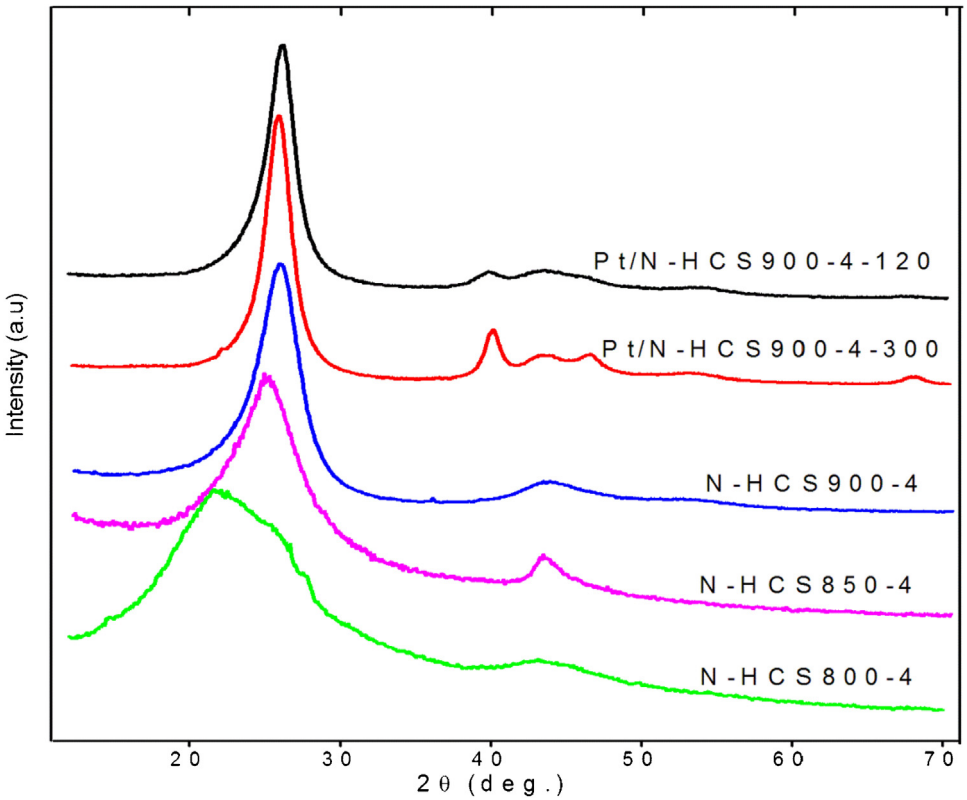

Fig. 2. XRD patterns for N-HCSs (prepared at different temperatures) and the Pt/N-HCS catalysts.

on the formation of a more highly graphitic carbon structure. The shell thickness also increased with reaction temperature.

3.1.4. Pt loaded N-HCSs

Pt was loaded onto the N-HCSs and the Pt/N-HCS materials were analyzed. The Pt metal content was determined by ICP-OES for Pt/N-HCS900-4-120 and shown to be 2.48%. A decrease in surface area was observed for Pt/N-HCS as compared with the N-HCS samples (Table 1).

The XRD patterns were recorded on the Pt supported materials. The data revealed that the Pt metallic phase (JCPDS file No-01-1194) was observed for Pt/N-HCSs. Thus the reduction process in Ar (5% H_2) atmosphere at 120 °C (Pt/N-HCS900-4-120) and 300 °C (Pt/N-HCS900-4 300) respectively was sufficient to generate the Pt metal particles (Fig. 2). The average crystallite size of the Pt nanoparticles in the Pt/N-HCS900-4-120 and Pt/N-HCS900-4-300 catalysts were 2.8 nm and 4.8 nm as estimated by using the Scherrer equation (Fig. 2) [53].

TEM images of the samples show spherical hollow carbon spheres with Pt particles with controlled size and distribution; a TEM image of Pt/NHSC900-4-120 is shown in Fig. 3. The well dispersed Pt nanoparticles had a narrow particle-size distribution centered at $d = 2.8 \pm 0.4$ nm (consistent with data determined from the XRD analysis).

Many studies have been performed in which Pt has been bound to a range of C supports and in these studies functionalization of the surface with acid, hydroxyl and ketonic groups has been reported to provide the binding sites for Pt [10,36–48]. The functionalised support generated small particles and this impacted on the selectivity and activity of the Pt. Here we have shown (as seen by others) that doping of carbon can also give a good metal dispersion for the Pt metal particles.

The XPS survey scan of Pt/N-HCS900-4-120 showed signals for the elements C, N, O and Pt (Fig. S3) and the expanded spectra for N and Pt are shown in Fig. S4. The XPS N1s spectra can be deconvoluted into three peaks centered at 401.5 (22%), 400.1 (48%) and 398.7 (30%) eV respectively assigned to quaternary, pyrollic and pyridinic-N species [54,55]. It is not known if all, or some, of these N atoms are the key species that lead to the N-Pt interactions that are responsible for the enhanced Pt dispersion on the N-HCSs.

Pt XPS data shows two distinct sharp Pt ($4f_{7/2}$) and Pt ($4f_{5/2}$) peaks around 71.7 and 76.2 eV respectively for Pt/N-HCS900-4-120 (Fig. S4). These are typical values for Pt(0), indicating that the deposited Pt (after H_2 treatment) is in the metallic state [56].

3.2. Catalytic activity tests

The various Pt loaded N-HCS supports (prepared at different temperatures and after different synthesis times) were studied as catalysts for the cinnamaldehyde reduction reaction at 80 °C and 30 bar. The results of the catalytic studies (Table 2) show that Pt on the different N-HCS supports leads to similar high conversions with similar good selectivities [Pt/N-HCS800-4-120 (90%/75%), Pt/N-HCS850-4-120 (96%/76%), Pt/N-HCS900-1-120 (91%/78%)] and Pt/N-HCS900-2-120 (98%/79%)] that increased slightly with the N-HCS carbon deposition temperature and time. These results suggested the use of a high carbon deposition temperature and a long reaction time to investigate a set of catalysts in more detail i.e. the Pt/N-HCS900-4-120 catalyst.

Data were collected at different temperatures (25 °C/40 °C/60 °C/80 °C) and pressures (10 bar/20 bar/30 bar) and are plotted in Table 3 (see also Fig. 4). It is clearly seen that increasing both the pressure and reaction temperature shifts the cinnamaldehyde transformation reaction to higher conversion/selectivity. Pressure has less effect on the selectivity to cinnamyl alcohol than temperature. For example at 60 °C the conversion changed from 65 to 87% and the selectivity from 71% to 87% as the pressure changed from 10 bar to 30 bar. In contrast as the T

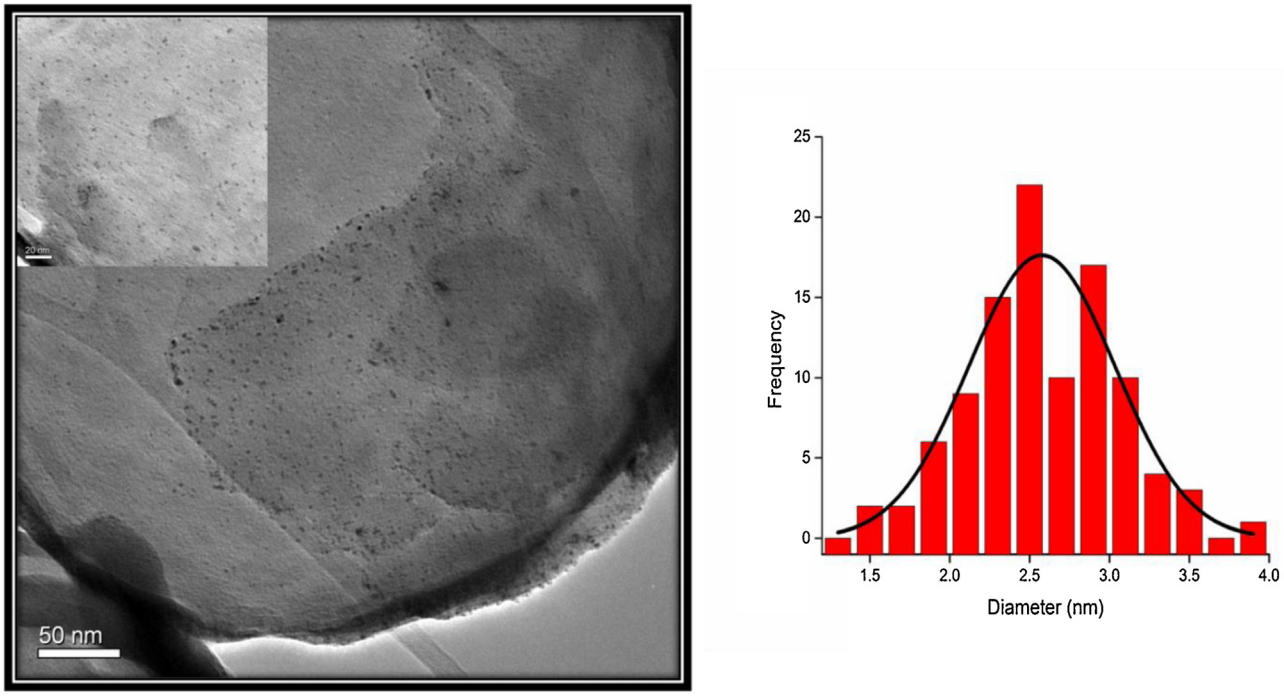

Fig. 3. TEM images of platinum nanoparticles on the Pt/N-HCS900-4-120 catalyst.

Table 2
The effect of catalyst synthesis parameters on the conversion of cinnamaldehyde and formation of cinnamyl alcohol [a].

Catalysts	Temperature °C	H^2(30 bar)			
		Select (%)			
		Conver(%)	A	B	C
Pt/N-HCS900-4-120	80	99	97	1	2
Pt/N-HCS900-4-300	80	85	95	3	2
Pt/N-HCS800-4	80	90	75	16	9
Pt/N-HCS850-4	80	96	76	14	10
Pt/N-HCS900-1-120	80	91	78	12	10
Pt/N-HCS900-2-120	80	98	79	10	11
Pt/HCS900-4-120	80	80	93	5	2

[a] Reaction conditions: cinnamaldehyde = 5 mL, catalyst weight = 0.2 g, solvent = isopropanol (30 mL), P = 30 bar; A = cinnamyl alcohol; B = 3-phenylprionaldehyde; C = 3-phenyl-1-propan-1-ol).

Table 3
The effect of temperature and pressure on the conversion of cinnamaldehyde and formation of cinnamyl alcohol[a].

Temperature °C	H_2 (10 bar)	Conver[a] select (%)			H_2 (20 bar)	Conver select (%)			H_2 (30 bar)	Conver select (%)		
	(%)	A	B	C	(%)	A	B	C	(%)	A	B	C
25	15	40	38	22	20	45	35	20	30	50	26	23
40	41	60	30	15	50	68	20	12	61	76	8	6
60	65	71	18	11	72	78	16	6	82	87	5	8
80	70	78	13	7	83	85	10	5	99	97	1	2

[a] Reaction conditions: cinnamaldehyde = 5 mL, catalyst weight = 0.2 g, solvent = isopropanol (30 mL), A = cinnamyl alcohol; B = 3-phenylprionaldehyde; C = 3-phenyl-1-propan-1-ol).

changed from 25 °C to 80 °C the conversion changed from 15 to 70% and the selectivity from 40% to 78% (at 10 bar). Importantly, at the higher pressures/temperatures little over reaction occurs to give 3-phenyl-1-propan-1-ol. Thus the formation of the by-products, 3-phenyl-1-propan-1-ol and 3-phenylpropionaldehyde was only favoured at low temperature and pressure. This is consistent with the model discussed by Durndell et al. [37].

To understand the origin of the activity/selectivity data further, other catalysts were tested.

i) The catalyst Pt/N-HCS900-4-300 (i.e. the same catalyst but heated at 300 °C for 2 h) gave a conversion of 85% cinnamaldehyde with 95% selectivity to cinnamyl alcohol. The lower activity is related to the presence of the larger (4.8 nm vs 2.8 nm) Pt nanoparticles.
ii) A catalytic reaction was performed with Pt/HCS900-4-120 (80 °C and 30 bar) and the data compared with Pt/N-HCS900-4-120 (both had similar particle sizes from TEM analysis). A lower conversion (80%) and selectivity (93%) for the undoped supported catalyst are noted (Fig. 5) indicating a measurable effect due

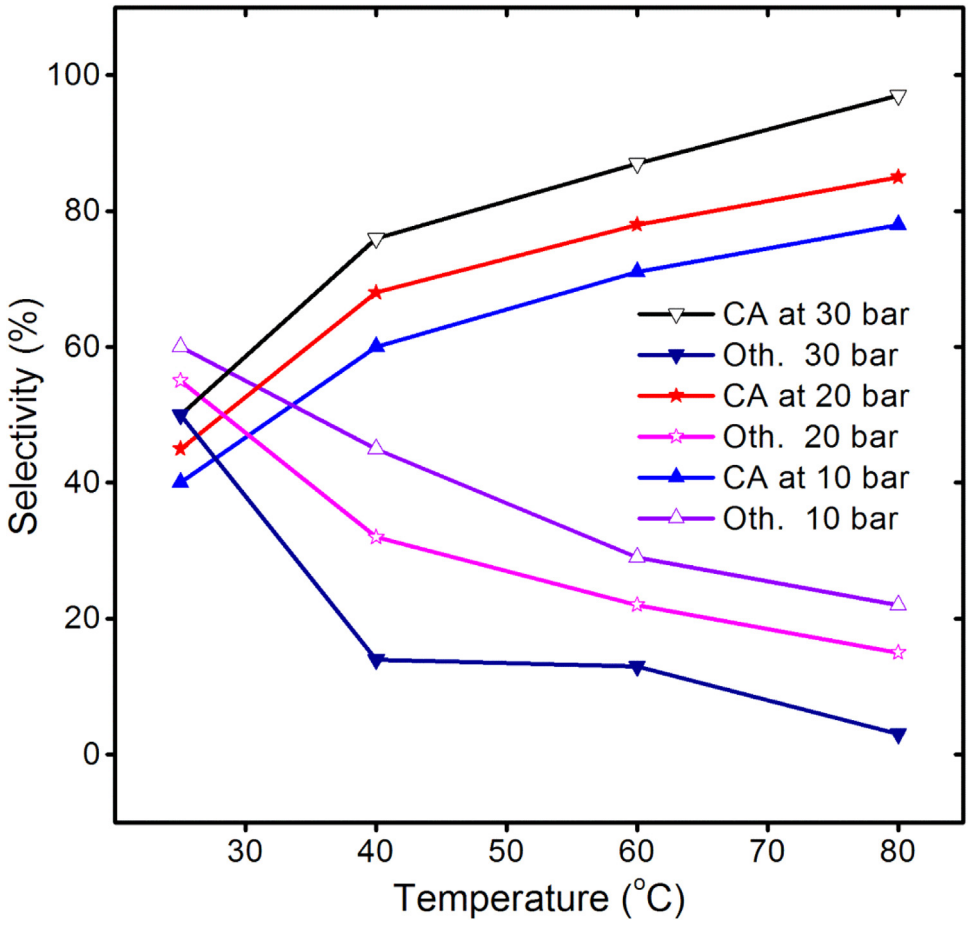

Fig. 4. Selectivity to cinnamyl alcohol (CA) and other (Oth) products as a function of temperature and pressure in the presence of Pt/N-HCS900-4-300 [reaction conditions: cinnamaldehyde = 5 mL, catalyst weight = 0.2 g, solvent = isopropanol (30 mL), Oth = 3-phenylprionaldehyde and3-phenyl-1-propan-1-ol].

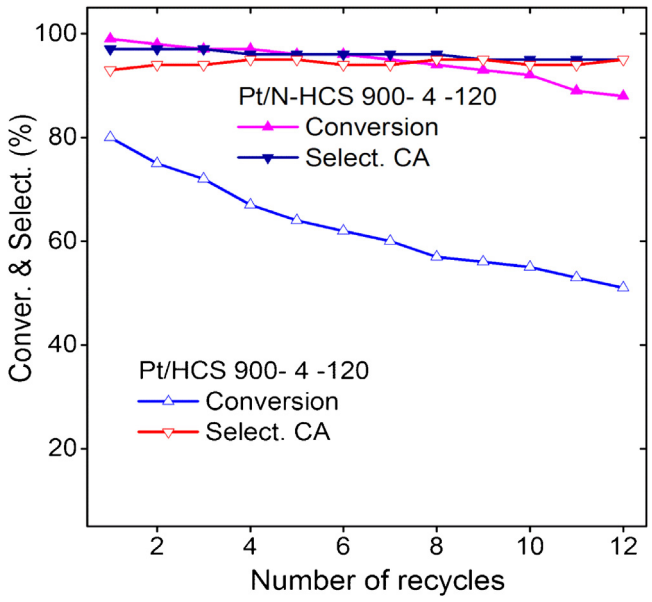

Fig. 5. The conversion of cinnamaldehyde and selectivity to cinnamyl alcohol (CA) over Pt/N-HCS900-4-120 and Pt/HCS900-4-120 catalysts before use (fresh), and over 12 recycles [reaction conditions: cinnamaldehyde = 5 mL, catalyst weight = 0.2 g, solvent = isopropanol (30 mL), reducing agent = H_2; P = 30 bar; temperature = 80 °C].

to the presence of the N atoms. This could be due to a surface 'polarity' effect associated with the N atoms [37].

A comparison with other reports on Pt supported on various other types of carbon reveals that excellent activity/selectivity results can also be achieved when the carbons are surface functionalized [36–49]. Our study reveals that N doping of the carbon can also lead to the selectivities/conversions described by others. Studies have been reported that suggest that the binding energies of Pt increase when Pt is supported on nitrogen doped carbon as compared with Pt supported on undoped carbon [57,58]. Thus, provided the surface area of the carbon is large enough (achieved in our case by removing the silica from the NHCSs) N doping provides an alternative to functionalization to generate good Pt-carbon interactions and resulting good catalyst conversions.

3.3. Catalyst stability test

Deactivation is an important factor when studying the long-term performance of a catalyst. Deactivation can occur by a number of processes including fouling, coking and leaching. At low temperatures, hydrocarbon coking reactions do not occur and any deposits are mainly derived from adsorbed reaction products and reactants.

Catalyst recycling experiments were performed with the Pt/N-HCS900-4-120 catalyst that was studied at 80 °C and 30 bar for 2 h. Fig. 5 shows that after reuse of the Pt/N-HCS900-4-120 twelve times, the conversion of cinnamaldehyde decreased from >99% to 90%, while the selectivity to the formation of cinnamyl alcohol

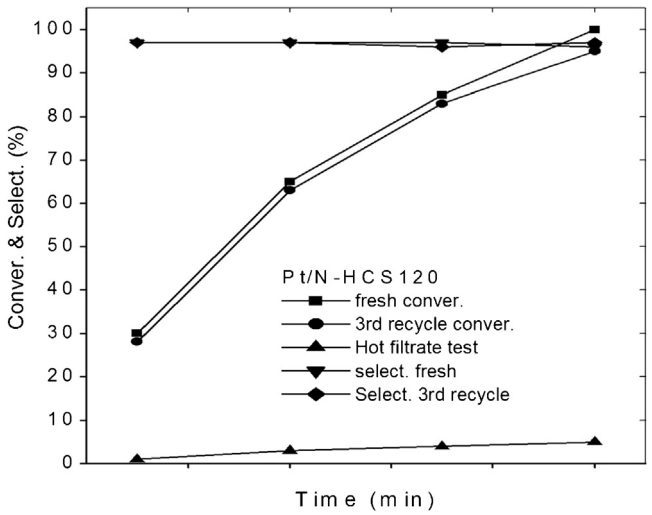

Fig. 6. The conversion of cinnamaldehyde and selectivity to cinnamlyl alcohol (CA) over Pt/N-HCS900-4-120 before use (fresh), and after a 3rd recycle. The filtered solution of the catalyst (hot filtrate; 3rd recycle) is also shown. The conversions are shown afer different time intervals [reaction conditions: cinnamaldehyde = 5 mL, catalyst weight = 0.2 g, solvent = isopropanol (30 mL); P = 30 bar; temperature = 80 °C].

remained constant (>97%) (Fig. 5). Chemical analysis of the used catalysts revealed that very little (if any) Pt (<2%) leached from Pt/N-HCS900-4-120. Indeed the Pt content was reduced from 2.49 wt% to ca. 2.42 wt% after use.

Furthermore, a catalytic reaction was carried out on the filtered solution (2 h at 30 bar and 80 °C) after separation of the catalyst from the reaction mixture (Fig. 6). The Pt/N-HCS900-4-120 filtrate gave < 4% conversion to cinnamyl alcohol. The data again suggests minimal, if any, Pt leaching. Indeed the main reason for the drop in conversion relates to the physical loss of the catalyst with repeated use.

Catalyst recycling studies were also performed on Pt/HCS900-4-120. The data reveal that while the selectivity remained constant at ca. 90% the conversion dropped with time. This drop is associated with catalyst leaching suggesting that the N doped support binds more strongly to the Pt particles.

3.4. Summary: N-HCSs as a support for the Pt catalyzed reaction

Many studies have appeared on the use of Pt supported catalysts for the cinnamaldehyde hydrogenation reaction. Our results are consistent with the many studies but provide added information on the process/reaction.

i) The use of carbon allows for excellent TEM/SEM contrast studies to evaluate the Pt particle size. While this was not the focus of this study, the particle size/conversion data are consistent with the reaction being dependent on the number of Pt atoms available for reaction. The selectivity is not affected by a change in particle size from 2.8 to 4.8 nm
ii) As the synthesis of the N-HCSs does not require the use of a catalyst, no contamination by residual metals (e.g. used to make CNTs) occurs and acid treatment to functionalize the C surface is not needed.
iii) The hollow sphere provides a means of making a carbon surface with a higher surface area than found for a solid sphere (SiO_2@C). This should lead to a better Pt dispersion.
iv) The role of the N doping of the HCS was to provide stronger support binding sites to the Pt. While the catalytic data shows some enhancement in activity (less relating to selectivity) on doping the HCSs, the advantage is readily seen in the catalyst reuse experiments where leaching is seen to be more pronounced from the undoped carbon.
v) The effect of pressure and temperature on the catalyst conversion/selectivity is seen to be consistent with the many other studies reported by others. The model proposed by Durndell et al. [37] involving 'surface crowding' is consistent with our data.
vi) The actual data compare with the best data reported to date for the selective conversion of cinnamaldehyde to cinnamyl alcohol

The study reveals that the Pt catalyst deposited on Pt/N-HCS900-4-120 showed good stability for the cinnamaldehyde reduction. Thus, the key factor revealed in these studies is that the Pt is well dispersed (small particles) and shows minimal leaching from Pt/N-HCS900-4-120 and is not sensitive to the formation of any carbonaceous residues deposited on the surface of the active metal species.

4. Conclusion

The data from the various studies indicate that the carbon shell deposited on the silica core is influenced by the reaction temperature and the reaction time. It appears that the reaction time has little influence on the C/N ratio. Indeed once the reactant has deposited on the silica the C/N ratio is not influenced further by the template. In the CVD reaction when using low reaction temperatures or short reaction times carbon pieces, broken spheres and deformed thin carbon shells were observed. At higher CVD temperatures (900 °C) and longer reaction times (4 h) the shell thickness increased and the N-HCSs had a superior graphitic nature.

XPS data recorded on Pt/HCS900-4-120 revealed that the N was inserted into the carbon with a high nitrogen content (8.6 wt%) and in the form of a range of species (quaternary, pyrollic, pyridinic). Well dispersed Pt nanoparticles with an average size of 2.8 nm were deposited on the N-HCS900-4 support. XRD and XPS studies revealed Pt was present in the metallic phase. Temperature and pressure studies were performed on Pt/HCS900-4-120 and the temperature effect was found to be more important than pressure in controlling the conversion and selectivity. The catalyst showed excellent conversion, recyclability and selective formation to the unsaturated cinnamyl alcohol. At 30 bar and a temperature of 80 °C excellent cinnamaldehyde conversion and selectivity to the unsaturated alcohol was achieved.

The study shows that N doping provides a good alternative to the use of carbon functionalization for binding Pt to carbon surfaces.

Acknowledgements

We thank the NRF, the Universities of the Witswatersrand and Johanesburg, and the DST-NRF Centre of Excellence in Strong Materials for financial support.

Appendix A. Supplementary data

Supplementary data associated with this article can be found, in the online version, at http://dx.doi.org/10.1016/j.apcata.2016.02.025.

References

[1] P. Chaturbedy, S. Chatterjee, R.B. Selvi, A. Bhat, M. Kavitha, V. Tiwari, A.B. Patel, T.K. Kundu, T.K. Maji, M. Eswaramoothy, J. Mater. Chem. B 1 (2013) 939–945.
[2] A.A. Deshmukh, S.D. Mhlanga, N.J. Coville, Mater. Sci. Eng. R Rep. 70 (2010) 1–28.
[3] X. Feng, C. Mao, G. Yang, W. Hou, J.-J. Zhu, Langmuir 22 (2006) 4384–4389.
[4] M. Inagaki, Carbon 35 (1997) 711–713.

[5] P. Serp, R. Feurer, P. Kalck, Y. Kihn, J. Faria, J. Figueiredo, Carbon 39 (2001) 621–626.
[6] P. Serp, J.L. Figueiredo, Carbon Materials for Catalysis, John Wiley & Sons, 2009.
[7] Y. Xia, B. Gates, Y. Yin, Y. Lu, Adv. Mater. 12 (2000) 693–713.
[8] M.-M. Titirici, M. Antonietti, Chem. Soc. Rev. 39 (2010) 103–116.
[9] M.-M. Titirici, A. Thomas, M. Antonietti, Adv. Funct. Mater. 17 (2007) 1010.
[10] H.C. Zeng, J. Mater. Chem. 21 (2011) 7511–7526.
[11] Q. Zhang, W. Wang, J. Goebl, Y. Yin, Nano Today 4 (2009) 494–507.
[12] J. Liu, S.Z. Qiao, J.S. Chen, X.W.D. Lou, X. Xing, G.Q.M. Lu, Chem. Commun. 47 (2011) 12578–12591.
[13] F. Su, X. Zhao, Y. Wang, L. Wang, J.Y. Lee, J. Mater. Chem. 16 (2006) 4413–4419.
[14] P. Valle-Vigón, M. Sevilla, A.B. Fuertes, Mater. Lett. 64 (2010) 1587–1590.
[15] X.-H. Li, M. Antonietti, Chem. Soc. Rev. 42 (2013) 6593–6604.
[16] Y. Li, T. Li, M. Yao, S. Liu, J. Mater. Chem. 22 (2012) 10911–10917.
[17] Z. Zhang, R. Zhang, C. Li, L. Yuan, P. Li, L. Yao, S. Liu, Electroanalysis 24 (2012) 1424–1430.
[18] F. Braghiroli, V. Fierro, M. Izquierdo, J. Parmentier, A. Pizzi, A. Celzard, Carbon 50 (2012) 5411–5420.
[19] A. Chen, Y. Yu, H. Lv, Y. Wang, S. Shen, Y. Hu, B. Li, Y. Zhang, J. Zhang, J. Mater. Chem. A 1 (2013) 1045–1047.
[20] Y. Liao, L. Gao, X. Zhang, J. Chen, Mater. Res. Bull. 47 (2012) 1625–1629.
[21] Y. Xia, Z. Yang, R. Mokaya, J. Phys. Chem. B 108 (2004) 19293–19298.
[22] Y.-M. Lu, H.-Z. Zhu, W.-G. Li, B. Hu, S.-H. Yu, J. Mater. Chem. A 1 (2013) 3783–3788.
[23] J. Jiang, Q. Gao, Z. Zheng, K. Xia, J. Hu, Int. J. Hydrogen Energy 35 (2010) 210–216.
[24] L. Guo, J. Zhang, Q. He, L. Zhang, J. Zhao, Z. Zhu, W. Wu, J. Zhang, J. Shi, Chem. Commun. 46 (2010) 7127–7129.
[25] X. Zhang, W. Zhang, Z. Yang, Z. Zhang, Front. Chem. Sci. Eng. 6 (2012) 246–252.
[26] S. Han, Y. Yun, K.-W. Park, Y.-E. Sung, T. Hyeon, Adv. Mater. 15 (2003) 1922–1925.
[27] X. Lai, J.E. Halpert, D. Wang, Energy Environ. Sci. 5 (2012) 5604–5618.
[28] Y. Wang, F. Su, J.Y. Lee, X. Zhao, Chem. Mater. 18 (2006) 1347–1353.
[29] K. Gong, F. Du, Z. Xia, M. Durstock, L. Dai, Science 323 (2009) 760–764.
[30] V. Ravat, I. Nongwe, N.J. Coville, ChemCatChem 4 (2012) 1930–1934.
[31] V. Ravat, I. Nongwe, R. Meijboom, G. Bepete, N.J. Coville, J. Catal. 305 (2013) 36–45.
[32] P. Claus, Top. Catal. 5 (1998) 51–62.
[33] M.J. Taylor, L.J. Durndell, M.A. Isaacs, C.M. Parlett, K. Wilson, A.F. Lee, G. Kyriakou, Appl. Catal. B 180 (2016) 580–585.
[34] C. Letizia, J. Cocchiara, J. Lalko, A. Lapczynski, A. Api, Food Chem. Toxicol. 43 (2005) 837–866.
[35] M.A. Vannice, B. Sen, J. Catal. 115 (1989) 65–78.
[36] K. Chizari, I. Janowska, M. Houllé, I. Florea, O. Ersen, T. Romero, P. Bernhardt, M.J. Ledoux, C. Pham-Huu, Appl. Catal. A 380 (2010) 72–80.
[37] L.J. Durndell, C.M. Parlett, N.S. Hondow, M.A. Isaacs, K. Wilson, A.F. Lee, Sci. Rep. 5 (2015).
[38] Z. Guo, Y. Chen, L. Li, X. Wang, G.L. Haller, Y. Yang, J. Catal. 276 (2010) 314–326.
[39] M.S. Ide, B. Hao, M. Neurock, R.J. Davis, ACS Catal. 2 (2012) 671–683.
[40] B.F. Machado, S. Morales-Torres, A.F. Pérez-Cadenas, F.J. Maldonado-Hódar, F. Carrasco-Marín, A.M. Silva, J.L. Figueiredo, J.L. Faria, Appl. Catal. A 425 (2012) 161–169.
[41] W.O. Oduro, N. Cailuo, K.M.K. Yu, H. Yang, S.C. Tsang, Phys. Chem. Chem. Phys. 13 (2011) 2590–2602.
[42] J. Serrano-Ruiz, A. López-Cudero, J. Solla-Gullón, A. Sepúlveda-Escribano, A. Aldaz, F. Rodríguez-Reinoso, J. Catal. 253 (2008) 159–166.
[43] Z. Sun, Z. Rong, Y. Wang, Y. Xia, W. Du, Y. Wang, RSC Adv. 4 (2014) 1874–1878.
[44] Z. Tian, C. Liu, Q. Li, J. Hou, Y. Li, S. Ai, Appl. Catal. A 506 (2015) 134–142.
[45] M.L. Toebes, T.A. Nijhuis, J. Hájek, J.H. Bitter, A.J. Van Dillen, D.Y. Murzin, K.P. de Jong, Chem. Eng. Sci. 60 (2005) 5682–5695.
[46] H. Vu, F. Gonçalves, R. Philippe, E. Lamouroux, M. Corrias, Y. Kihn, D. Plee, P. Kalck, P. Serp, J. Catal. 240 (2006) 18–22.
[47] Y. Wan, Y.-L. Min, S.-H. Yu, Langmuir 24 (2008) 5024–5028.
[48] B.-H. Zhao, J.-G. Chen, X. Liu, Z.-W. Liu, Z. Hao, J. Xiao, Z.-T. Liu, Ind. Eng. Chem. Res. 51 (2012) 11112–11121.
[49] R. Zheng, M.D. Porosoff, J.L. Weiner, S. Lu, Y. Zhu, J.G. Chen, Appl. Catal. A 419 (2012) 126–132.
[50] W. Stöber, A. Fink, E. Bohn, J. Colloid Interface Sci. 26 (1968) 62–69.
[51] J.X. McDermott, J.F. White, G.M. Whitesides, J. Am. Chem. Soc. 98 (1976) 6521–6528.
[52] H.A. Tayim, M. Kharboush, Inorg. Chem. 10 (1971) 1827–1828.
[53] A. Patterson, Phys. Rev. 56 (1939) 978.
[54] M.-C. Huang, H. Teng, Carbon 41 (2003) 951–957.
[55] X. Jin, V.V. Balasubramanian, S.T. Selvan, D.P. Sawant, M.A. Chari, G.e.Q. Lu, A. Vinu, Angew. Chem. 121 (2009) 8024–8027.
[56] G. Zhang, D. Yang, E. Sacher, J. Phys. Chem. C 111 (2007) 565–570.
[57] L. Jia, D.A. Bulushev, O.Y. Podyacheva, A.I. Boronin, L.S. Kibis, E.Y. Gerasimov, S. Beloshapkin, I.A. Seryak, Z.R. Ismagilov, J.R. Ross, J. Catal. 307 (2013) 94–102.
[58] X. Xie, J. Long, J. Xu, L. Chen, Y. Wang, Z. Zhang, X. Wang, RSC Adv. 2 (2012) 12438–12446.